Catena 250 (2025) 108797

Contents lists available at ScienceDirect

Catena

journal homepage: www.elsevier.com/locate/catena

Deccan volcanic bole beds (Greater Mumbai, India): New insights on their nature and evolution based on micromorphology

Seema Singh [a,*], Ajay Kumar [a], Soumyajit Mukherjee [b], Charu Sharma [a], Anshul Dhiman [a]

[a] *Department of Geology, Panjab University, Chandigarh 160 014 India*
[b] *Department of Earth Sciences, Indian Institute of Technology Bombay, Powai, Mumbai, Maharashtra 400 076, India*

ARTICLE INFO

Keywords:
Deccan Basalt
Palaeosol micromorphology
Ferralsols
Late Cretaceous

ABSTRACT

The globally occurring flood basalt volcanic eruptions consist of interbasaltic layers within successive lava flows, and are commonly referred as red '*bole beds*' due to their dominantly red colour. These bole beds are *in-situ* layers within successive lava flows, making them reliable geologic proxy tools. These beds also represent short to prolonged hiatus in volcanic activity and subsequent landscape stability. The Indian Deccan traps comprising several bole bed layers constitute one of the world's largest flood basalt volcanic provinces. The Deccan bole bed studies have already been done based on geochemistry but researchers reached no consensus on their nature and origin, presumably due to lack of detailed and systematic micromorphology. In this regard, ~ 100 cm thick buried bole bed profile in Kharghar hill (greater Mumbai, India) has been investigated for detailed morphological and micromorphological studies along-with selective geochemical studies. Pedoplasmation features include development of specific voids and microstructure, b-fabrics, bioturbation features and one or more types of pedofeatures. Systematic micromorphology shows that the investigated buried bole bed profile were mature palaeosols formed on pyroclastic deposits. Significant biodiversity under ustic soil moisture regimes existed and resulted in the formation of ferralsols. A greater impact of andosolization on ferralsols is interpreted before onset of successive basalt lava flow. A combination of morphological, micromorphological and geochemical results indicate presence of oxidizing environment under high temperature and acidic soil conditions during pedogenesis. Thus, systematic bole bed micromorphology is pre-requisite for understanding of surficial conditions during quiescence in volcanism. These results are a first step towards detailed such investigations in future for various exposures of bole beds during different phases of Deccan volcanism. Further, compiled multi-proxy dataset will prove significant to compare similar studies done in global, contemporaneous volcanic bole beds.

1. Introduction

The Earth's geologic history witnessed flood basalt volcanic eruptions at specific geologic time periods. The Siberian (~ 250 Ma), Newark (~ 200 Ma), Karoo (~ 190 Ma), Antarctic (~ 170 Ma), Rajmahal (~ 110 Ma), Madagascar (~ 90 Ma), Deccan (~ 65 Ma), Ethopian (~ 35 Ma) and Columbia River (~ 16.5 Ma) flood basalt eruptions are some of the major ones in the Earth's history (Ernst, 2014). Though continental flood basalts are spread over millions of km^2 on the Earth surface, they formed within rather short geologic time periods. Self et al. (1997) documented that majority of the individual eruptions in flood basalts occurred within a million year or even less. This makes them important repositories for palaeoclimate and palaeoenvironment reconstructions within definite time intervals of the Earth's evolutionary history. The continental flood basalt studies further become significant due to their association with major extinction events (McLean, 1985; Rampino and Stothers, 1988; Haggerty, 1996; Courtillot and Gaudemer, 1996; Olsen, 1999; Wignall, 2001; White and Saunders, 2005; Sayyed, 2014 and references therein). Amongst various silicate rocks, basalts act as a major sink of the atmospheric CO_2 as they are considered to undergo extensive chemical weathering, depending on various factors, in particular distinct climatic conditions (Prasad et al., 2025 and references therein).

Flood basalts consist of interflows, dominantly red coloured strata/layers within successive lava flows. These interbasaltic layers are commonly known as '*bole beds*' or red layers. They are the marker horizons/beds formed on flow contacts, in between successive lava flows. These have been considered even as Martian soil and sediment analogues based mainly on their spectral signatures and chemical

* Corresponding author.
E-mail address: geoseema05@yahoo.co.in (S. Singh).

https://doi.org/10.1016/j.catena.2025.108797
Received 28 January 2024; Received in revised form 21 January 2025; Accepted 30 January 2025
Available online 4 February 2025

compositions (Kletetschka et al., 2000; Wänke et al., 2000; Barrón and Torrent, 2002a, 2002b; Craig et al., 2017). This is especially true for the Deccan volcanic bole beds of the peninsular India (Gavin et al., 2010, 2012; Greenberger et al., 2012; Craig et al., 2017). Also, bole beds represent hiatuses in basalt lava flow emplacement suggesting the episodic nature of volcanism and subsequent interaction with the Earth's surface processes. Therefore, study of bole beds provide information on palaeoclimate, palaeoweathering, landscape stability, nature of surface processes and palaeoenvironment conditions during temporal breaks between large-scale volcanic events. Further, these are buried strata/units which got preserved in original within successive lava flow units, thereby indispensable geologic proxy tools. Emphasis on such interbasaltic strata (i.e. bole beds/red layers) studies gained pace in the late nineties and is continuing. Notwithstanding, the nature and origin of these kinds of bole beds have remained controversial till date. For example, these could be palaeosols formed on basalts during the quiescence periods, baked/fritted layers; regolith/weathering surfaces including paleo-laterites, or simply the sedimentation units.

The Deccan plateau/traps of the peninsular India covers > 500,000 km^2 across mainly the western and the central India (Mukherjee et al., 2017). These basalts consist of several conspicuous red to brown coloured interflow strata/layers. Despite several works done on bole beds from the Deccan trap, the nature and their origin remain unsolved, perhaps due to lack of systematic micromorphological studies. On the other hand, such detailed studies have been carried out for bole beds between basalt flows at worldwide volcanic occurrences (e.g., Spinola et al., 2017). The micromorphological studies are well established as reliable tools in solving several complex geological problems (e.g., Stoops et al., 2010, 2018; Singh et al., 2015, Singh et al., 2017). Therefore, bole beds exposed in the Deccan volcanic hill in the greater Mumbai (Maharashtra, India) have been explored for such buried profiles within successive basalt flows. The hypothesis of this study is that the buried bole bed profile is a palaeoweathered surface with or without significant pedogenesis, which formed during periods of insignificant or no volcanic activity. Thus, the major objective from this study is to identify the nature of bole beds using systematic sequential morphological and micromorphological studies to develop greater understanding on their genesis during the then prevailing geological conditions.

2. Study area

2.1. Geology & stratigraphy

Several researchers have studied the geology and stratigraphy of the Deccan large igneous province (DLIP)/ Deccan Traps (e.g., reviews in Mukherjee et al., 2017). Researchers have also compiled distribution of compound and simple flows in the Deccan trap- the former occurs in western part of the Deccan trap (Mahoney, 1988; Bondre et al., 2006; Duraiswami et al., 2012 and others). Both types of flows can be mapped over many square km (Ghodke, 1979). Further, simple and compound flows can be distinguished in the field by the grain size and phenocryst mineralogy and may be aphyric or contain pyroxene, olivine, and/or plagioclase phenocrysts (Beane et al., 1986). Detailed stratigraphy of DLIP in Western Ghats of India has been discussed by Beane et al. (1986). They documented 10 formations, which fall in to three subgroups of the Deccan Basalt Group based on their overall field characteristics and chemical and isotopic composition. The three subgroups from the oldest to the youngest in the Deccan Basalts of western Ghats include the Kalsubai Subgroup, the Lonavala Subgroup and the Wai Subgroup (Beane et al., 1986). The Kalsubai Subgroup comprises the lower 5 formations. In younging direction, these are Jawhar, Igatpuri, Neral, Thakurvadi and Bhimashankar formations. The Lonavala Subgroup overlies the Kalsubai Subgroup and comprises the Khandala and the Bushe formations. The Wai Subgroup is composed of upper three formations namely (from bottom to top), the Poladpur, the Ambenali, and the Mahabaleshwar. Misra et al. (2014; therein Table 1 and Fig. 2) discussed the stratigraphy and tectonics of the DLIP of Maharashtra, India. Fig. 1 shows that the study area is located at the western part of DLIP of the greater Mumbai region (Maharashtra, India). Detailed compilation of geology and stratigraphy including lithostratigraphy and chemostratigraphy has been done by Misra et al. (2014, refer to their Table 1). Following Misra et al. (2014), the studied section in the Kharghar Deccan hill of Mumbai falls in the Upper Ratangarh Formation (equivalent to the Bhimashankar Formation chemostratigraphically) of Kalsubai Subgroup. Lithologically, the Ratangarh Formation consists of dense aphyric to phyric flows with moderately porphyritic pahoehoe flows. In general, the Bhimashankar Formation consists of compound flows having coarse-grained amygdaloidal basalt with densely packed and up to 1 cm size plagioclase glomerocrysts (Beane et al., 1986).

2.2. Materials & methods

Identification and characterization of bole bed palaeosols have been done by recording horizon-wise field/ morphological properties following Retallack et al. (1988). These were logged in the field and features, viz., soil structure, colour, texture, mottles, horizon boundaries, nodules, roots have been described as per Retallack et al. (1988) and Soil Survey Staff (1992). Munsell Soil Colour Chart by Kollmorgen Instruments Corporation (Mnsell, 2000)) has been used to name colours. Undisturbed, *in-situ* bole-bed samples were collected in Kubiena tin boxes of dimension 10 cm * 12 cm * 16 cm and 5 cm* 6 cm * 8 cm during field investigations for micromorphological studies. Systematic bulk sampling has been done for geochemical analyses. Thin-sections were prepared as per Miedema et al. (1974), Jongerius and Heintzberger (1975 and references therein). However, hardened bole-bed and basalt rock samples were sectioned as per Carver (1971). These were described according to the system proposed by Stoops (2003; 2021). All the micromorphological/ thin-section observations have been done under Carlz Zeiss and Radical polarizing microscopes at the Department of Geology (Panjab University, Chandigarh, India).

Major elements were analyzed to quantify the chemical weathering and other pedogenic changes in the parent material (Birkeland, 1984). Major and selective trace elements have been determined by using Laser Ablation Inductively Coupled Plasma Mass Spectrometry (LA-ICP-MS of model iCAP RQ by Thermo Scientific, USA, 2019) at the Sophisticated Analytical Instrumentation Facility (SAIF) and the Department of Geology, Panjab University, Chandigarh (India) following Shapiro (1975), Bandemer and Schaible (1944), Eggins (2007). The data obtained is presented as oxides since the major balancing anion is oxygen. The whole-rock samples were analyzed for major oxides. Major oxide data were converted to molecular mass from the weight percentage and for all of the presented geochemical functions, the molar rather than oxide equivalent for a given element is shown. Most proxies include ratios of different elements used for weathering and pedogenic processes based on various proxies as summarized in supplementary Table 1 along-with corresponding references.

3. Results & interpretations

3.1. Morphological & micromorphological

The investigated bole bed profile reveals characteristic morphological and micromorphological pedogenic features (Figs. 2-6). Fig. 2 shows complete bole bed, buried profile logged along with the lower (stratigraphically older) and upper (stratigraphically younger) basalt units, and these are designated as P, B1 and B2, respectively. Whereas the upper boundary contact of P with the overlying basalt unit (i.e. B2) is abrupt and smooth, the lower boundary contact with B1 is clear and broken (Fig. 2a). The logged ~ 100 cm thick P-profile is subdivided from bottom to top (stratigraphically up) into P1 and P2 layers based on diagnostic morphological features (e.g. colour, structure and compactness; Fig. 2b). The topmost part of P2, designated as $P2_1$, is ~ 15–25 cm

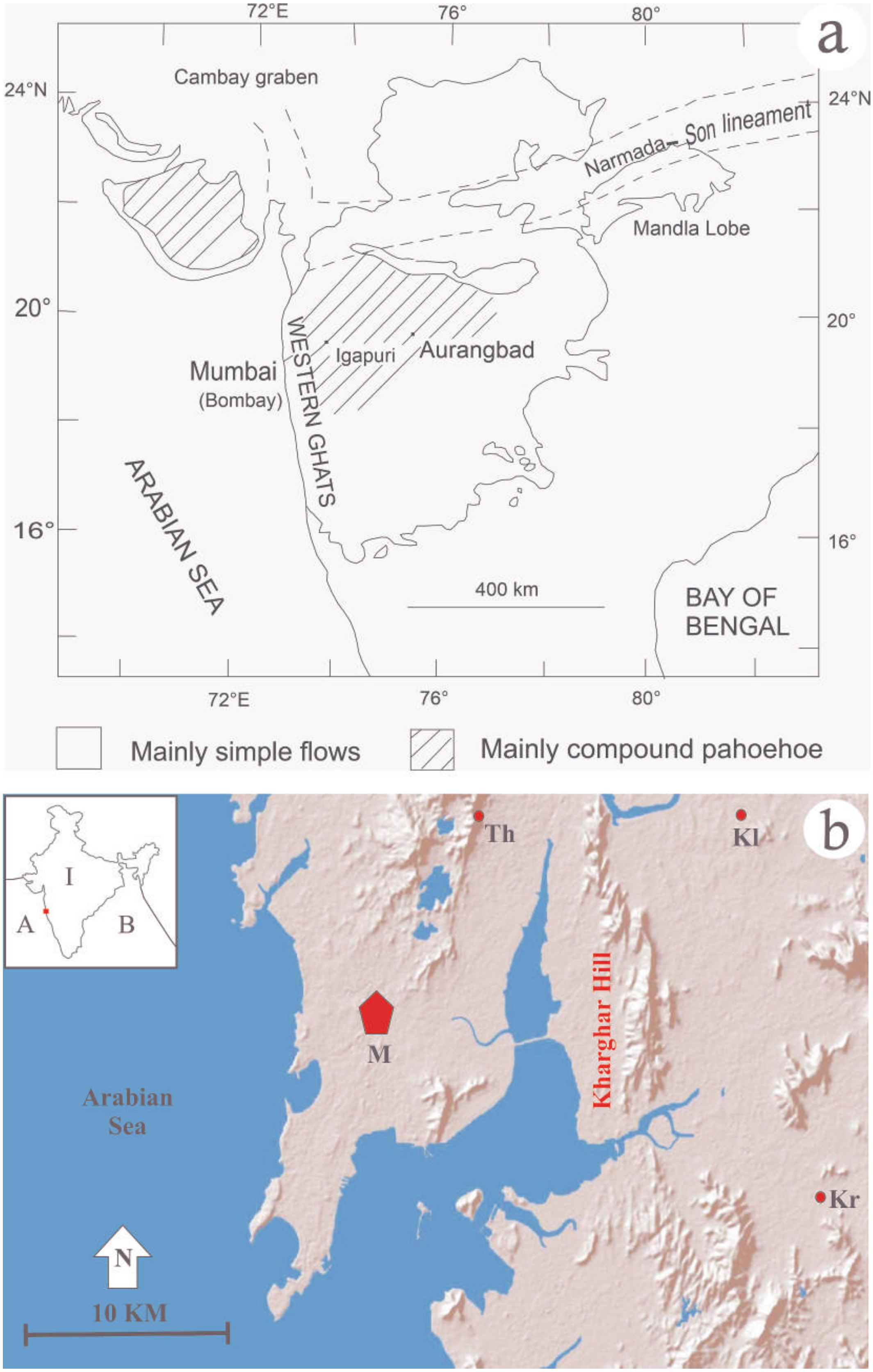

Fig. 1. (a) Map showing Deccan traps with simple and compound flows (after Ross et al., 2005 and references therein). (b) Surface Topographic Image showing location of Kharghar hill (Mumbai), wherein the bole bed section was logged. M: Mumbai, TH: Thane, KL: Kalyan, KR: Karjat. Inset map shows Mumbai region (red dot) in India. Therein I, A, B respectively stands for India, Arabian Sea and Bay of Bengal.

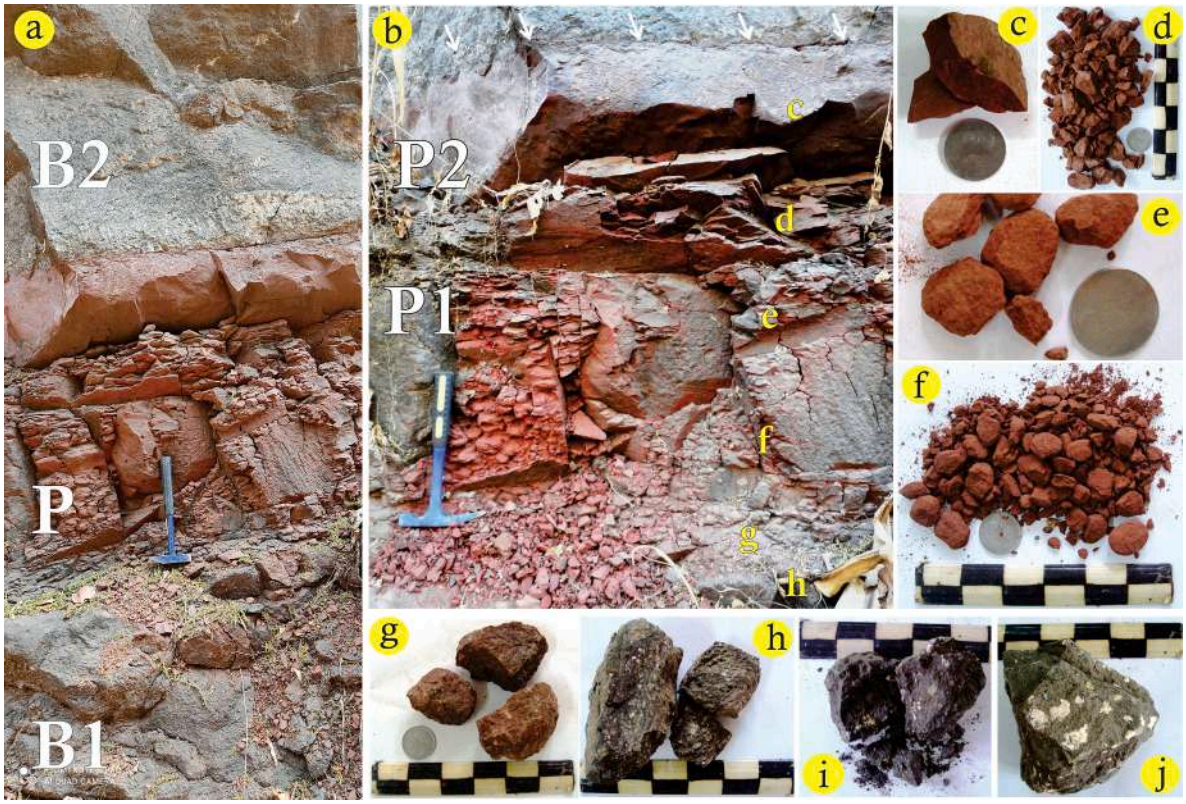

Fig. 2. (a) Representative field photograph showing logged bole bed buried section (named as P) underlain and overlain by the Deccan flood basalts (i.e. designated respectively as B1 and B2) in the Kharghar Hill, Mumbai (India). Note the abrupt and smooth upper contact between the overlying flood basalt unit and the bole bed whereas broken lower contact with the weathered flood basalt unit. (b) The bole beds are further divided in to two major layers from bottom to top, namely P1 and P2 layers based on characteristic morphological features. Herein c, d, e, f, g, h are locations in the P layer showing larger view/bulk samples from top to bottom in the respective figures (c), (d), (e), (f), (g), (h). (i) Representative photograph of bulk sample of weathered basalt unit, B1. (j) Representative photograph of bulk sample from the overlying basalt unit, B2. Geological hammer used as scale is ~ 30 cm. Each black and white rectangle of scale is 1 cm. Coin used as scale has ~ 2 cm diameter.

thick and is hard, compact and dark reddish grey (10R 3/1) to greyish brown in colour. It shows very thick platy structure and grades into lower layer, designated as $P2_2$, with clear, wavy boundary contact. $P2_2$ is ~ 20–25 cm thick and is hard and dusky red (10R 3/4). It shows thin platy structure as well as fine blocky structure, and grades into lower layer $P1_1$, with gradual, wavy boundary contact which is in specific based on variation in structure from the platy to subangular to subrounded blocky peds. $P1_1$ is ~ 40–50 cm thick, dusky red (10R 3/3) in colour and shows fine to medium, subangular to subrounded blocky structure. The transition from $P1_1$ to the lower layer $P1_2$ is diffuse and broken. $P1_2$ is ~ 15–25 cm thick, dark brown to dusky red (10R 2.5/2) towards top but grades in to reddish green towards bottom-most part. It shows weakly developed and coarse, platy to blocky structure. $P1_2$ grades into lower layer (i.e. the top part of B1 viz., $B1_1$), with clear but irregular boundary contact. $B1_1$ is friable, purplish to dark brownish green, and consists of blocky to columnar structure. On other hand, the underlying layer is comparatively compact and greenish grey in colour.

A number of micromorphological features indicative of *in-situ* pedogenesis (Stoops, 2003; Federoff et al., 2010; Stoops et al., 2010, 2018) have been identified. Pedoplasmation features include development of voids and microstructure, b-fabrics, bioturbation features and one or more types of matrix and/ or intrusive pedofeatures. The nature and degree of development of these micromorphological features vary from top to bottom in the studied P profile (Figs. 3-6).

The topmost $P2_1$ red layer immediately below the B2 layer shows glassy micromass and absence of voids. However, vesicles are present and filled with glass. In general, this part consists of spherical aggregates, which are properly welded. Micromass is pale to bright yellow and shows predominantly undifferentiated b-fabric but at places speckled to striated b-fabrics are also present. Further below this $P2_1$ layer, voids are present, having dominance of spheroidal aggregates/ peds with compound packing voids. This resulted in moderately to well-developed granular microstructure, which is however reworked at places. Amongst other types of voids, some irregular vughs and channels have been observed. Vughs are present along-with thin, unaccommodated planar voids and vary between very fine to fine sand size. Coarse fraction is moderately sorted and predominantly varies from medium sand-size to very fine sand-size. Coarse fraction consists of all kinds of phenocrysts/clasts, which show various degrees of weathering/alteration resulting in alteromorphs, wherein shape of primary mineral is preserved at places. Sideromelane/scoria grains, glass shards are abundant but some plagioclase laths and few basaltic/volcanic xenoliths as well as pumice grains have been identified in the coarse fraction. Glass shards show varied sizes and commonly with platy to cuspate shapes besides irregular. The altered glass shards show a range of colours, such as brown, red, black, yellow, orange and dark brown. These are commonly altered to palagonite and other clay minerals, except some fresh glass shards. Likewise, except few fresh scoria grains, others are completely altered to alteromorphs, though preserving traces of primary shape at many places. Both altered and fresh plagioclase mineral grains are identifiable. Likewise, few big grains of both altered and fresh basaltic xenoliths have been observed. Micromass colour varies from dark brown to light brown and largely comprises altered coarse material/minerals, alteration products including clays, iron-oxides as well as sesquioxides. Amongst b-fabrics, speckled, striated and undifferentiated b-fabrics have been identified. Coatings and hypocoatings of only micromass material (including alteration products comprising clay and Fe-Mn oxides) around coarse grains and voids are present and

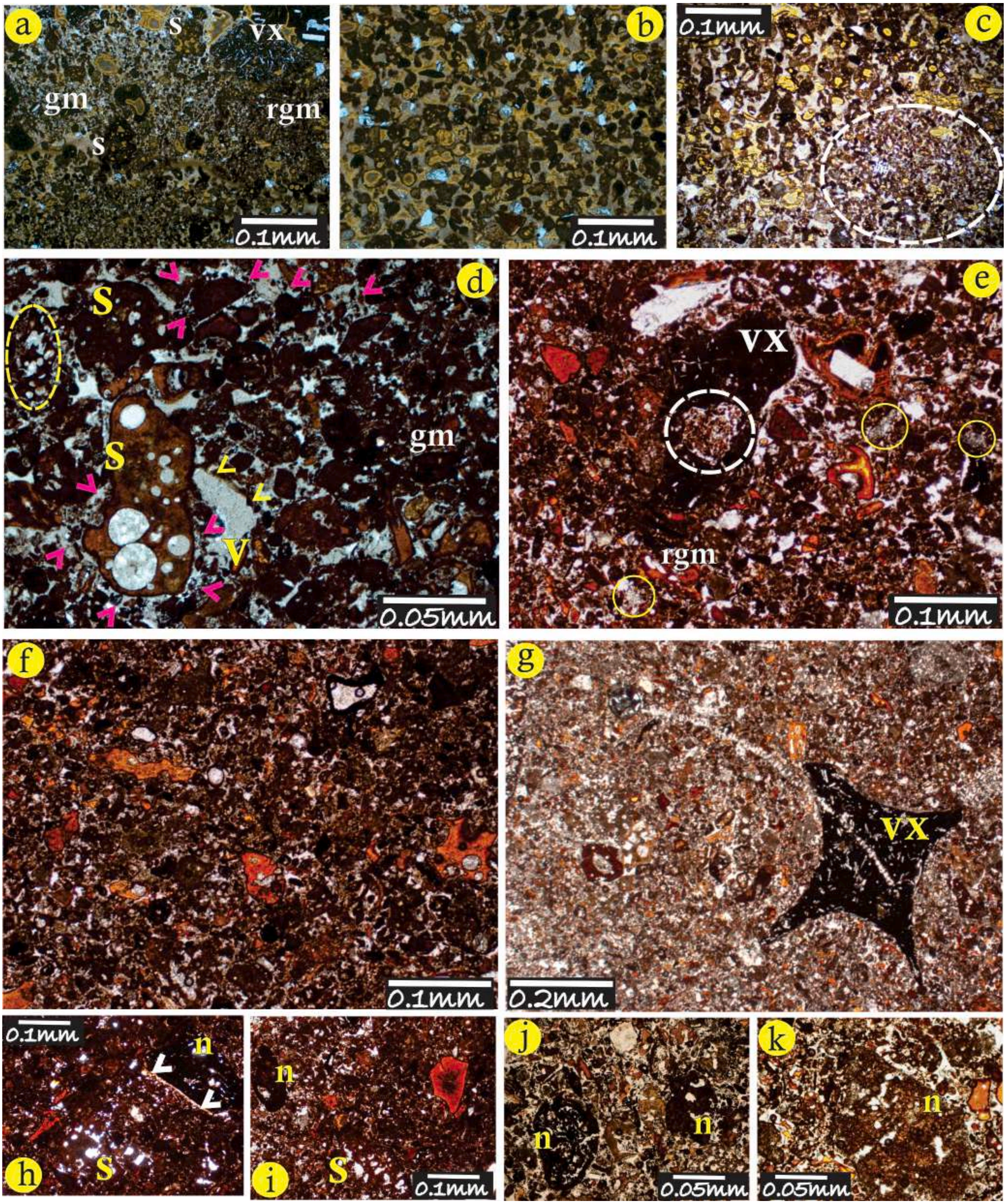

Fig. 3. Representative photomicrographs showing major pedoplasmation features in the (a-c): topmost i.e. immediately below B2 unit, part of $P2_1$ layer; (d-g): middle part of $P2_1$ layer; (h-k): bottommost part of $P2_1$ layer. All photomicrographs in PPL. Representative pedofeatures are shown with the key: VX- volcanic xenolith; S- scoria; gm-granular microstructure; rgm-reworked granular microstructure due to bioturbation; n-nodule; V-void; yellow dashed ellipse- strongly altered scoria; white dashed ellipse- faunal pedofeature; pink arrows- coating/arrangement of micromass material; white arrows- striated b-fabric; yellow arrows- illuvial clay coating.

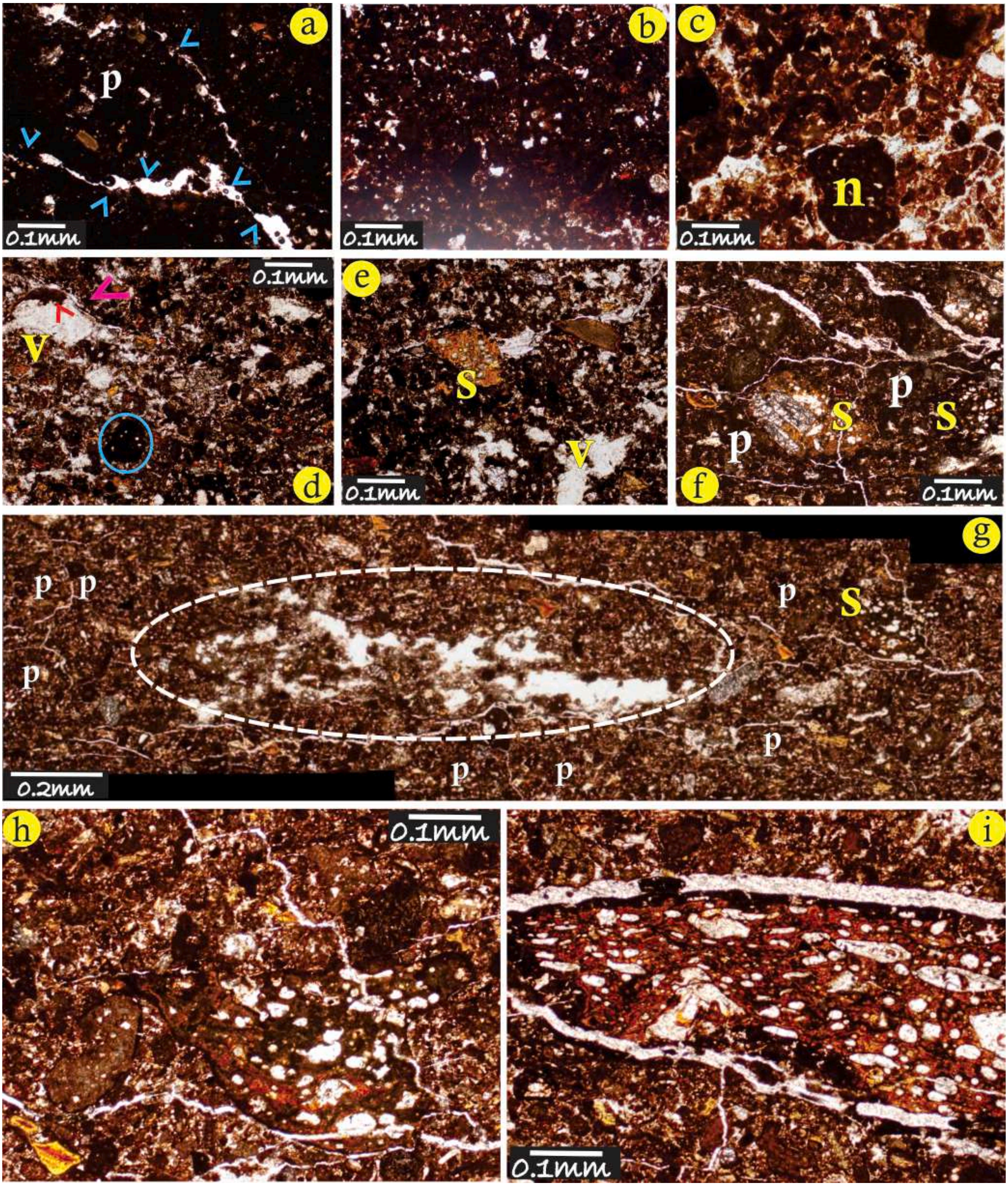

Fig. 4. Representative photomicrographs showing major pedoplasmation features in the (a-c): topmost part of $P2_2$ layer; (d), (e): lower part of $P2_2$ layer; (f-i): $P1_1$ layer. All photomicrographs in PPL. Representative pedofeatures are shown with the key: P- soil ped; S- scoria; n-nodule; V-void; white dashed ellipse- faunal pedofeature; pink arrow- coating/arrangement of micromass material; blue arrow- faunal void/pedofeature; red arrow- ferruginous coating.

laminated coatings are absent. Further, moderately impregnated sesquioxide to ferruginous nodules have been observed. In general, nodules are orthic and show typic, aggregate to dendritic internal fabric. The most common of these are reworked altered material (i.e. ferruginous) from sideromelane. The diagnostic pedofeatures are abundant faunal pedofeatures. Representative photomicrographs from the $P2_1$ layer are shown in Fig. 3.

The $P2_2$ layer shows dominance of fine to medium, spheroidal aggregates/peds with compound packing voids, resulting in moderately to well-developed granular microstructure. Further the bottom-most part

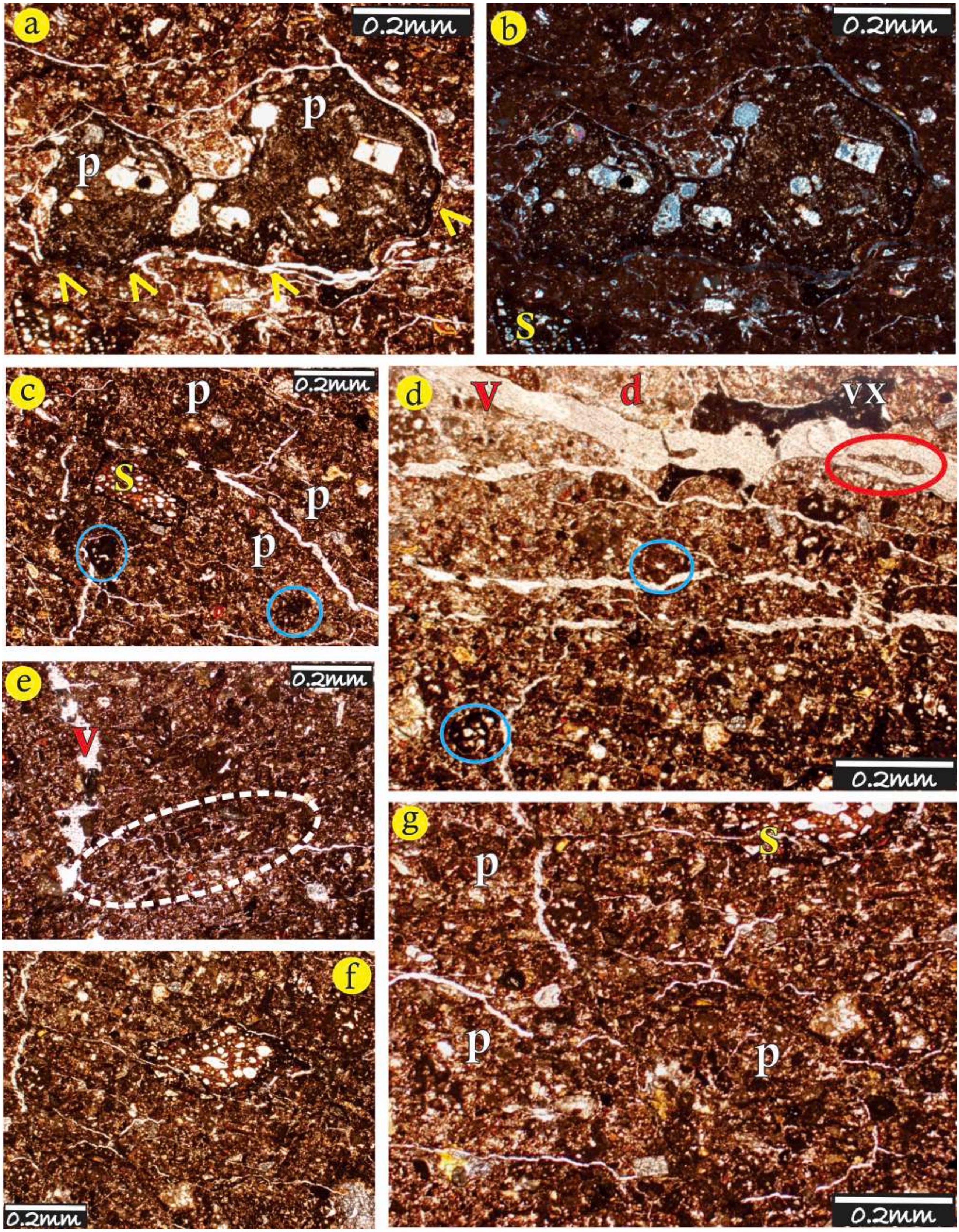

Fig. 5. (a-g): Representative photomicrographs showing major pedoplasmation features in the P1$_1$ layer. All photomicrographs in PPL except fig. b (XPL). Representative pedofeatures are shown with the key: VX- volcanic xenolith; S- scoria; P- soil ped; n-nodule; V-void; d- depletion pedofeature; red ellipse- micromass infilling; blue ellipse- completely altered scoria to sesquioxide segregation; yellow arrows- coating/plastering of micromass material along void.

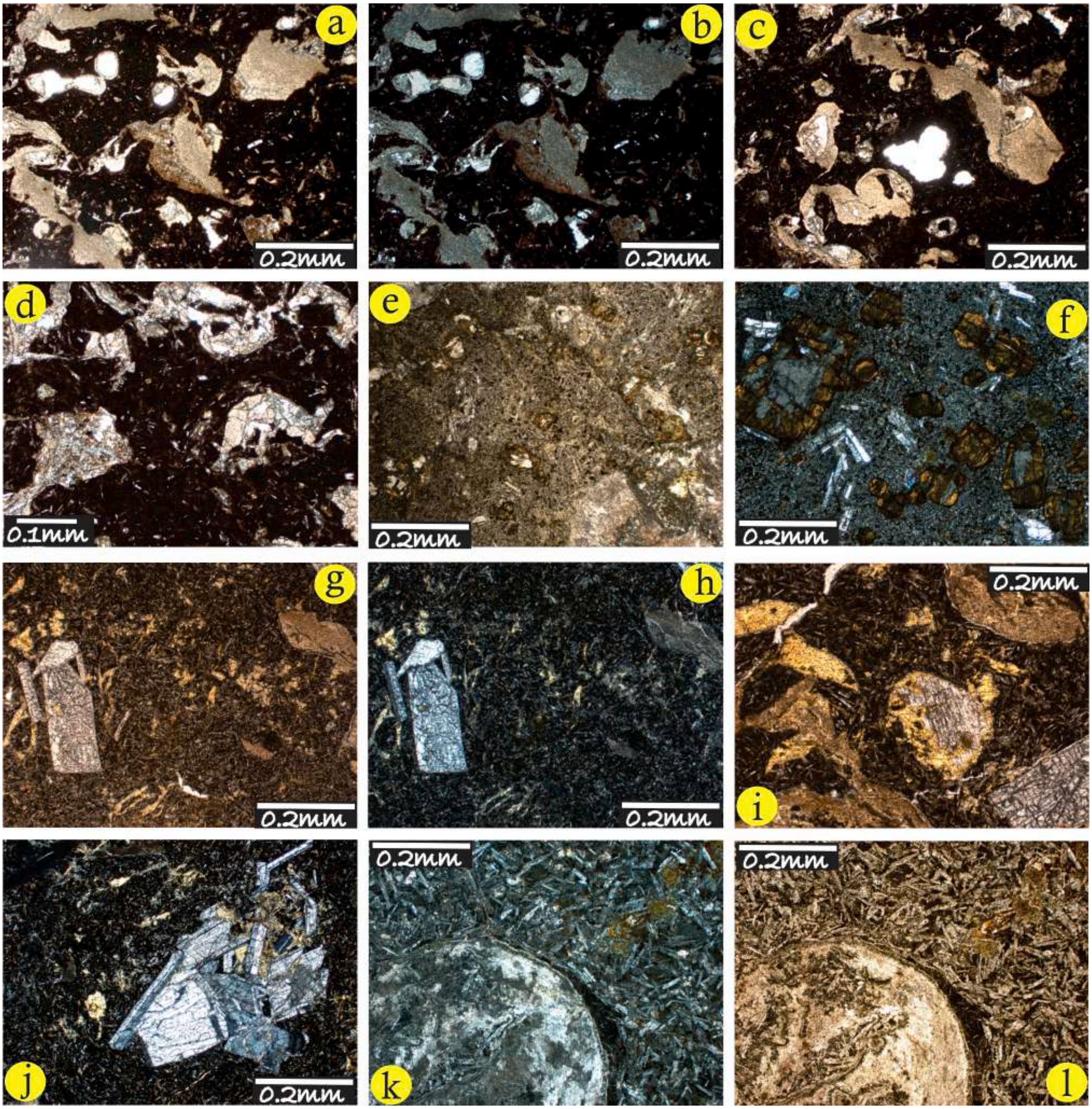

Fig. 6. Representative photomicrographs showing rock fabric in the (a-d): $P1_2$ layer; (e), (f): topmost part i.e. $B1_1$ of B1 unit; (g-j): B1unit; (k-l): B2 unit. Photomicrographs in PPL are a, c, d, e, g, i, l and others are in XPL.

of this layer shows weakly developed, coarse blocky microstructure with unaccommodating peds (Fig. 4a). Voids vary from highly irregular vughs, channels, along-with thin to thick, highly irregular and largely unaccommodated planar voids (Fig. 4a-e). The coarse fraction is poorly sorted, largely sub-rounded and ranges between very coarse to fine sand-size. It consists of all kinds of altered phenocrysts including abundant scoria, sideromelane/glass shards, some fresh to altered plagioclase grains and few pumice grains. In general, coarse fraction is predominantly altered except some plagioclase and volcanic fragments. Micromass colour is dark brown and comprises altered coarse material/minerals, alteration products including clays, iron-oxides as well as sesquioxides. Amongst b-fabrics, undifferentiated b-fabric is dominant but weakly developed speckled to striated has also been observed. Coatings and hypocoatings of micromass material as well as crystalline material (including alteration products) around coarse grains and voids have been observed at places. Coatings and hypocoatings of neoformed clay in completely altered volcanic material/fragments is easily identifiable. Further, loose discontinuous infilling of clay and micromass material as well as presence of reworked material has been noticed. Some moderately impregnated sesquioxide to ferruginous nodules/segregations, have been observed. Representative photomicrographs for this layer are shown in Fig. 4. It is important to note that amongst all pedofeatures, the faunal pedofeatures are dominant throughout the P2 layer.

The $P1_1$ layer of the profile is distinct due to presence of abundant voids and moderately to well-developed blocky peds. This layer dominantly shows subangular to subrounded blocky microstructure, wherein majority of peds are moderately separated, accommodated to partially accommodated and peds greatly vary in size (fine sand to very coarse sand-size). However, intrapedal spheroidal-granular peds varying in size from silt to fine sand have been identified. In particular, planar voids dominate and the thick ones accompany complexly arranged channel/ chamber parts. Planar voids vary in thickness, show straight to zigzag planes and are partially accommodated to unaccommodated (Fig. 4f-i; 5). Another distinct feature of this layer is the presence of larger scale (up to 4 mm) bioturbation/ faunal features/ peds (Fig. 4g). Coarse fraction is poorly sorted and varies between very coarse to fine sand-size. Coarse fraction largely comprises completely altered to moderately altered scoria/sideromelane/glass shards and plagioclase grains wherein the largest size variation (i.e. very coarse to fine sand size) is shown by scoria whereas plagioclase laths are dominantly of fine sand-size. Further, few volcanic/basaltic xenoliths have been noticed and except the plagioclase laths, which are completely fractured/ cracked and filled with alteration products like clay and iron oxides, the scoria and volcanic fragments are present in both. Some are slightly altered but majority comprise largely/ completely altered forms. Micromass colour is predominantly brown and comprises altered coarse material/minerals and alteration products. Amongst b-fabrics, at places speckled to granostriated b-fabric but predominantly undifferentiated b-fabric with cloudy limpidity has been observed. Some coatings and hypocoatings in altered grains and voids consist of micromass material, neoformed clay and iron-manganese oxides but absence of any laminated coatings. Similarly, loose, incomplete clay and micromass material infillings have been identified.

The transition from $P1_1$ to lower layer $P1_2$ is diffuse and broken. $P1_2$ is ~ 15–25 cm thick, shows colour variation from dusky red (10R 2.5/2) to reddish brown in the top whereas dark grey to brownish green in the bottom. Micromorphology of $P1_2$ layer differs much from the overlying $P1_1$ layer. The top part of $P1_2$ layer shows few voids but significant vesicles, which are either isolated (oval to circular in shape) or coalesced and are also either empty or filled with minerals and at places deformed. Coarse fraction comprises altered phenocrysts, dominantly of plagioclase and augite, besides the secondary minerals in vesicles. Micromass is very dark brown, shows undifferentiated b-fabric and the fine fraction comprises amorphous or cryptocrystalline colloidal components wherein some fine, plagioclase laths can also be observed. Unlike the top layers (i.e. $P2_1$, $P2_2$, $P1_1$) this layer lacks scoria (irrespective of altered or unaltered) grains or any other grains/clasts.

Both the red layers, P1 and P2, except bottom-most of P1 (i.e. $P1_2$) consist of coarse material comprising altered to unaltered clasts and the size is < 2 mm. The coarse material comprising glass decreases from the topmost P2 (i.e. $P2_1$) to $P1_1$. Scoria/sideromelane grains are common but the abundance of altered scoria increases from $P2_1$ to $P1_1$. In the $P1_1$ layer some fresh/ slightly weathered scoria and plagioclase grains can be easily identified. Coarse material is highly weathered in the $P1_1$ layer compared to the P2 layer. Also the pyroclasts are somewhat flattened, giving a current-flow appearance in the P1 layer. Volcanic glass is common and unweathered to partially weathered in the P2 layer whereas almost completely weathered and less in abundance in the $P1_1$ layer. Also, the glass and plagioclase grains as coarse materials are highly fractured/fissured and filled with sesquioxides/ iron oxides in the $P1_1$ layer. Both very dark, nearly opaque (i.e. tachylite) and dark variety of basaltic glass have been observed in the P2 and the $P1_1$ layers. Further, more weathered groundmass from P2 to $P1_1$ layer has been observed. Scoria/sideromelane grains are weathered to palagonite-like allophane alteromorphs in a manner similar to those described by Gerard et al. (2007).

3.2. Geochemical studies

Geochemical plots related to Section 2.2 (and Supplementary Table 1) using major element and trace element values are shown in Fig. 7. The calculated values of Chemical Index of Weathering, CIW (Maynard, 1992; Harnois, 1988) in the studied bole bed profile (P-layer) along-with basalt unit (i.e. B1) range from 72.34 to 81.75, wherein the lowest value is 72.34 which is from $P1_2$ layer, sampled at ~ 95 cm. The highest calculated CIW value is 81.75 at depth ~ 115 cm and forms the $B1_1$ layer of B1 (Fig. 7, plot 2). Besides CIW, Plagioclase Index of

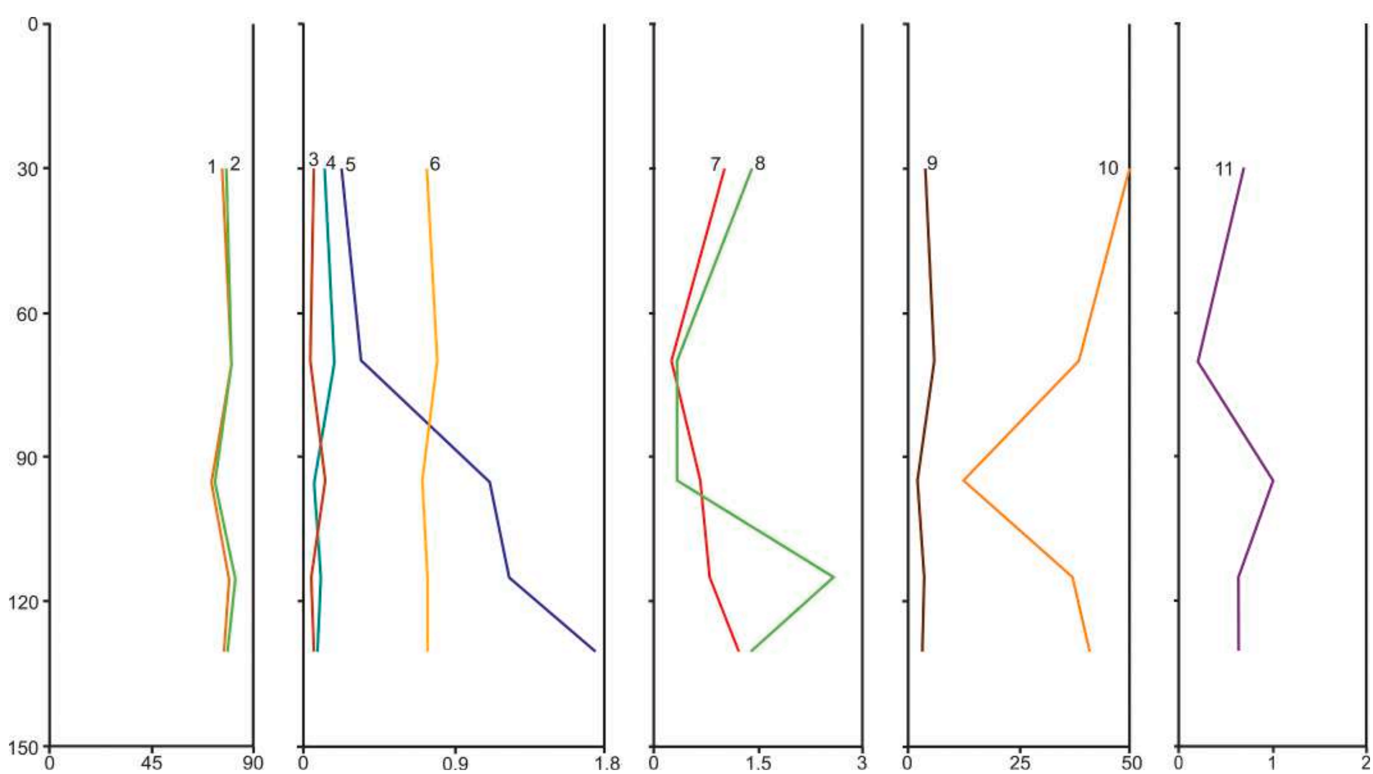

Fig. 7. Geochemical plots in the logged bole bed profile (i.e. P) and the underlying basalt unit (i.e. B1), wherein the y-axis shows the depth in cms and on the x-axis plots 1, 2, 3, 4, 5, 6, 7, 8, 9, 10, 11 are respectively PIA, CIW, Provenance, Clayeyness, Gleization, Hydrolysis, Na/Ti, K/Ti, Ca/Ti, Mg/Ti, U/Th. Referred to supplementary Table 1 for more details.

Alteration (PIA) has been calculated (Fedo et al., 1995), which ranges from 71.43 to 80.37 and the lowest value 71.43 is of $P1_2$ layer, sampled at $\sim$ 95 cm whereas the highest value 80.37 has been found to be of samples at $\sim$ 70 cm and $\sim$ 115 cm depths which are respectively from $P1_1$ and $B1_1$ layers of the logged profile (Fig. 7, plot 1). The higher (i.e. $\geq$ 80) CIW and PIA calculated values in the layers $P1_1$ (middle part of bole bed profile) and $B1_1$ (topmost part of basalt unit) indicate significant alteration/weathering to form pedogenic B-horizon. The other process, which gives an idea of weathering and/or pedogenesis is the hydrolysis. It is calculated either by measuring the accumulation of Al with respect to Si (i.e. clayeyness) or the loss of base cations with respect to Al (Sheldon and Tabor, 2009), the former being documented as more robust pedogenic proxy tool for interpreting hydrolysis if combined with micromorphological observations. The clayeyness value (Ruxton,1968; Sheldon and Tabor, 2009) is lowest (i.e. 0.067) of samples at $\sim$ 95 cm depth from $P1_2$ layer whereas highest (i.e. 0.177) of samples at $\sim$ 70 cm depth from $P1_1$ layer indicating the latter be designated as B-horizon (Fig. 7, plot 4). The calculated values using loss of base cations with respect to Al in the studied profile vary from the lowest 0.701 value at $\sim$ 95 cm sample from $P1_2$ layer and highest 0.797 value at $\sim$ 70 cm sample from $P1_1$ layer in a manner similar to clayeyness (Fig. 7, plot 6). In general, no significant variation in its value except $P1_1$ layer samples. Herein it needs mention that researchers have widely used loss of base cations with respect to Al (i.e. $\sum$Bases/Al) ratio in palaeosols for a variety of purposes irrespective of some potential issues in using this in metasomatically altered palaeosols, as shown and compiled by Sheldon and Tabor (2009). For example, $\sum$Bases/Al ratio of 0.5 has been statistically considered a dividing value between Alfisols ($>$ 0.5) and Ultisols ($<$ 0.5) (Sheldon and Tabor, 2009). Therefrom, the studied bole bed profile fall under Alfisol category due to $>$ 0.5 values of $\sum$Bases/Al ratio in the profile. However, no such classification is adopted in the present work due to limitations associated in very ancient soils compared to modern soil classifications.

Leaching is another significant process to interpret pedogenesis. Leaching has been calculated using a base loss ratio where the abundance of a given base is divided by the abundance of Ti and this approach has been documented best for palaeosols formed on igneous and metamorphic rocks (Sheldon and Tabor, 2009). Each of the base cation (i.e. Na, K, Mg, Ca) divided by Ti has been plotted as a function of depth in the profile (Fig. 7, plots 7–10). The values for the Na/Ti ratio, range from 0.266 to 1.2, with the lowest and highest values occurring at a depths 70 cm (i.e. $P1_1$ layer) and 130 cm (i.e. B1 layer) respectively. The K/Ti values range from 0.333 to 2.6, with the lowest value occurring at depths 70 cm and 95 cm from P1 layer and whereas highest value at a depth of 115 cm from $B1_1$ layer. The Mg/Ti values range from 12.333 to 49.4, with the highest value occurring at a depth of 30 cm (i.e. $P2_2$ layer) and the lowest value occurring at depth 95 cm (i.e. $P1_2$ layer). The Ca/Ti ratio ranges from 2.222 to 6, with the highest value occurring at a depth of 70 cm (i.e. $P1_1$ layer) and the lowest value occurring at depth 95 cm (i.e. $P1_2$ layer). In general, the base cations should be leached during weathering at normal pH conditions and Ti accumulated (Sheldon and Tabor, 2009). Depending on climate, topography and pH conditions, the monovalent and divalent cations in a profile show varied leaching behavior from top to bottom for a soil formed on same parent material. Leaching behavior of monovalent and divalent cations in the studied bole bed profile is variable and is discussed in section 4 along with morphological and micromorphological features for proper interpretations.

The gleization ratio (Fe^{2+}/Fe^{3+}) has been calculated in order to understand oxidation conditions during pedogenesis (Sheldon and Tabor, 2009). In the logged profile the gleization values range from 0.222 to 1.717, with the highest value occurring at a depth of 130 cm (i.e. B1 unit) and the lowest value occurring at depth 30 cm (i.e. $P2_2$ layer) (Fig. 7, plot 5). Researchers have documented that gleization ratio is different for various unweathered parent rocks. For example, Sheldon (2003) demonstrated that the unweathered Columbia flood basalts show gleization ratio $>$ 2; whereas the palaeosols formed under well-drained conditions typically show gleization ratio $\ll$ 0.5. This was attributed due to greater oxidizing conditions during soil formation (Sheldon and Tabor, 2009). Researchers have widely demonstrated higher gleization values during weathering/pedogenesis occurring under reducing/hydromorphic/ waterlogged conditions than those formed under well-drained, oxidizing conditions. In the studied profile, abruptly higher gleization values in the lower part of profile ($>$ 100 cm) compared to the upper part of profile have been found. Therefore, this clearly indicates change in redox conditions from reducing to oxidizing during formation of bole bed palaeosol. Another line of evidence for the intense weathering under oxidizing conditions during formation of bole bed palaeosol is the pattern shown by U/Th ratio. In the studied profile, the U/Th values range from 0.194 to 1.01, with the highest value occurring at a depth of 95 cm (i.e. $P1_2$ layer) and the lowest value occurring at depth 70 cm (i.e. $P1_1$ layer) (Fig. 7, plot 11). Researchers have shown that the U/Th ratio is constant with depth in a profile under no significant pedogenesis and redox gradient because both U and Th are relatively immobile except during intense weathering conditions (Condie et al., 1995; Li, 2000; Sheldon and Tabor, 2009). Sheldon and Tabor (2009) documented that under strong redox gradient and intense weathering conditions, U is leached away during pedogenesis but Th remains because only U^{6+} is soluble under oxidizing conditions. This results in lower values of U/Th ratio in the upper horizons of soil than the parent material and this pattern is well reflected in the studied bole bed profile.

This is further supported from the Ti/Al ratio, which provides information on pH conditions during weathering/pedogenesis besides being used as a reliable indicator of provenance as well as to infer parent material homogeneity (Rye and Holland, 2000; Sheldon and Tabor, 2009 and references therein). In the studied profile, the Ti/Al values range from 0.038 to 0.132, wherein the highest value occurring at a depth of 95 cm (i.e. $P1_2$ layer) and the lowest value occurring at 70 cm depth (i.e. $P1_1$ layer) (Fig. 7, plot 3). In the studied profile, the Ti/Al values are not constant with depth indicating change in pH conditions during pedogenesis/weathering. Sheldon and Tabor (2009) documented that Ti/Al are most mobile under acidic pH conditions. Therefore, the ratio should potentially shift from the parent material value depending on the pH conditions. This can be well observed in the P-layer, wherein the $P1_2$ layer shows significantly higher values compared to the top layers. Further, in a manner similar to the compilation done by Sheldon and Tabor (2009), the Ti/Al values in the studied profile is $\ll$ than 0.1, suggesting well-developed palaeosol formed on basalt – like mafic parent material.

3.3. Profile characterisation of bole bed-cum-palaeosol

The interbasaltic layer (red bole beds designated as P) between two successive basalt units has been investigated in detail using morphological, micromorphological and geochemical studies. Fig. 8 shows how the studied $\sim$ 100 cm bole bed profile has been subdivided based on compilation of diagnostic morphological, micromorphological and geochemical results. The bottom-most part of $P1_2$ red layer is designated as ABb horizon, which actually formed on weathered and weakly pedogenised scoriaceous lava, followed by basaltic lapilli tuff. The latter may have contributed as parent material of the buried palaeosol on the red bole bed resulting in formation of Bw horizon at successive stages. The lapilli tuff shows hypocrystalline and mesocrystalline crystallinity and the texture is porphyritic comprising predominantly basaltic mineral phenocrysts embedded in very dark brown undifferentiated micromass/groundmass. The buried Bw horizons from top to bottom are Bwb1, Bwb2 and Bwb3 for the $P2_1$, $P2_2$ and $P1_1$ red layers of bole bed, respectively. A lithic discontinuity (LD) is suggested between 2ABb and Bwb3 due to absence of any pyroclastic material in the former besides other pedoplasmation differences, in particular characteristic c/f material, microstructure and pedofeatures. All the Bw horizons formed on predominantly unconsolidated pyroclastic material (i.e. tephra).

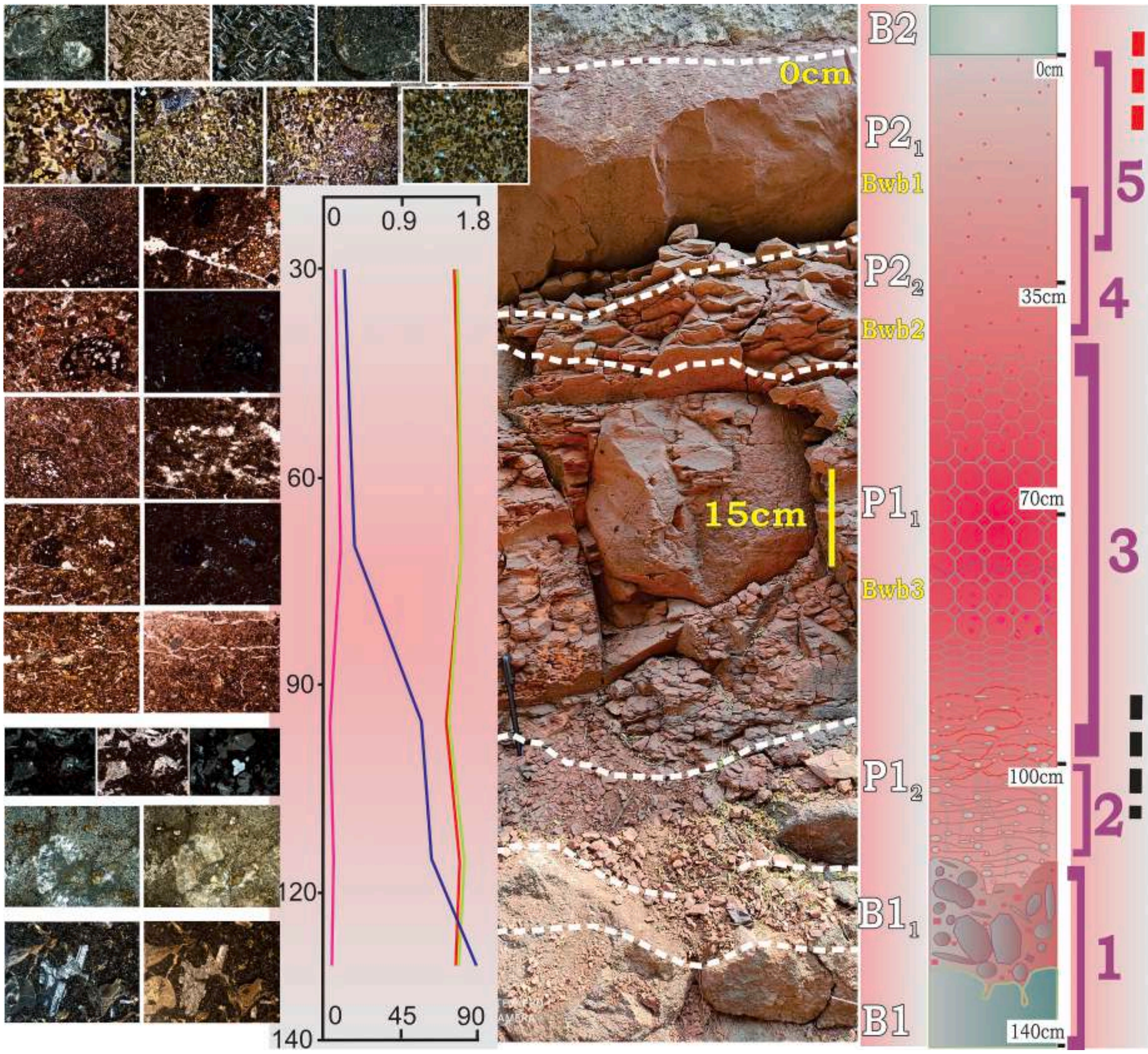

Fig. 8. Compilation of results based on characteristic morphological, micromorphlogical and geochemical in the logged bole bed profile (i.e. P) and the underlying basalt unit (i.e. B1) to understand the nature and genesis of Deccan bole bed. The left side of the figure consists of systematic in-depth arrangement of thin-section and selective geochemical proxies along-with the logged field photograph. Whereas on the right side of logged section, the various stages (i.e. 1–5) of evolution and nature of bole bed in to palaeosol horizons has been given. Stage 1 comprises weathering and pedogenesis of B1 forming basalt alterite, wherein the topmost (i.e. B1$_1$) forms the alloterite and the lower part forms the isalterite (Dhiman et al., 2024). Stage 2 includes weathering and weak pedogenesis of scoriaceous lava deposit and is represented by P1$_2$ red layer (i.e. ABb horizon). Stages 3, 4 and 5 represent the successive stages resulting in formation of bole bed mature palaeosol profile resulting in Bw horizons. The bottommost i.e. Bwb3 is the subsurface horizon of the ferralsol. The topmost i.e. Bwb1 shows greater influence of andosolization before emplacement of next basalt lava deposit (i.e. B2). The dotted black and red lines on the extreme right side respectively indicate lithic discontinuity and overlying basalt lava (i.e. B2) heating effect on the topmost part of P2$_1$ layer as discussed within text.

Further, the pyroclastic material is similar in mineralogical composition, consisting of both weathered/altered pyroclasts and fresh pyroclasts, which consists of scoria/sideromelane/basaltic xenoliths/glass shards/ tachylite and plagioclase laths. However, the size and sorting vary from Bwb1 to Bwb3. The bottom-most Bwb3 shows poorly sorted coarse material but extensively altered coarse material and groundmass as well as greater presence of variety of pedoplasmation features compared to Bwb1 and Bwb2 horizons. This indicates that Bwb3 is the most mature soil, subsurface horizon which is further supported by the calculated geochemical pedogenic indices (e.g. CIW, PIA, Clayeyness, etc.). Whereas finer size and greater percentage of fresh grains in coarse material dominate the topmost horizon Bwb1. Nonetheless, pedoturbation remains the dominant process in all these horizons based on diagnostic faunal pedofeatures and is discussed in detail in the succeeding section.

4. Discussions: Nature and evolution of *bole bed-cum-palaeosol*

Researchers reached no consensus on the nature and origin of bole beds in the Deccan basalts. For example, Wilkins et al. (1994) suggested that these beds are weathered pyroclasts based on geochemical studies. Widdowson et al. (1997) concurred their pyroclastic origin and further suggested those are the fossilized weathered paleosurfaces. The bole beds have also been reported as mostly weakly developed ancient soils (Ghosh et al., 2006; Sayyed and Hundekari, 2006; Srivastava et al., 2015). The red, green and brown coloured bole beds have been assigned different origins. Ghosh et al. (2006) suggested that the green varieties are equivalent to the andosols whereas the red bole beds are palaeolaterites. These authors reconstructed intense precipitation during Deccan volcanism based on geochemical results. Sayyed and Hundekari (2006) attributed red and green bole beds for different protoliths. They also documented that the bole beds may not have undergone intense weathering and long-term pedogenesis when compared to the modern soils developed on the Deccan basalts. Gavin et al. (2010) demonstrated baking of these Deccan bole beds to ∼ 600 °C. Shrivastava et al. (2012) documented intense weathering, ∼ 5-fold higher than that operating on the parent lava flows, of these bole beds under wet and dry climate cycles in the past. Contrarily Srivastava et al. (2012) refuted pedogenesis/lateritization of these bole beds and suggested deposition of baked/unbaked sediments by shallow streams or laterally migrating channels. They interpreted that a ponding condition formed green bole beds and the following brown boles by detrital lacustrine or floodplain depositional environments. Study of detailed mineral magnetism and diffuse reflectance spectroscopy (DRS) led Srivastava et al. (2015) to conclude that green, brown and red boles formed from the transitional baking environments under hydrous-anhydrous conditions and pedogenic processes. Their study suggested less heating and aerobic pedogenic environment for the brown and the green boles and high temperature oxidative environment for the red boles. Further, Srivastava et al. (2018) documented these bole beds as the product of basalt weathering based on trace element studies.

Recently, Singh et al. (2021, 2022) on the basis of textural and mineralogical studies, demonstrated possible pedogenesis of these bole beds. Very recently, Sriwastava et al. (2023) focused on clay mineralogy of bole beds and envisaged pedogenesis and palagonitization processes responsible for clay formation in these bole beds. They documented kaolinite and smectite clays in both red and grey bole beds, which is in contrary to Craig et al. (2017). Even though different coloured bole beds (e.g. yellow, red and green) are chemically similar to each other and to the underlying basalt from which they have been weathered, show different clay minerals (Craig et al., 2017). Nonetheless, Sriwastava et al. (2023) based on clay mineralogy interpreted presence of oxidizing conditions at low temperatures and fluctuating wet and dry seasons. Further, these authors documented incipient stage of weathering/pedogenesis resulting in formation of saprolite despite high degree of leaching. This brief review shows that despite significant existing works on bole beds in India, their nature and genesis remains unresolved. One plausible reason is the lack of detailed, sequential micromorphological investigations, which are indeed essential to establish nature and genetic evolution of geological deposits in complex geological settings (Singh et al., 2015, Singh et al., 2017). Previous studies have documented Deccan bole beds as largely the weathering products of underlying basalt and in general indicated presence of wet and dry, oxidizing conditions for red bole beds.

In this work, systematic and detailed micromorphological investigations of the bole beds proved significant in revealing the nature of the bole beds. The investigated Deccan bole beds are identified as palaeosols formed on pyroclastic deposits rather than directly on the underlying basalts, as parent material. Also, combination of detailed morphological and micromorphological results with geochemical results comprising weathering and pedogenic indices suggest use of geochemical parameters alone with caution in such geological deposits. This is further elaborated in succeeding paragraphs. We do not question the significance of such geochemical indices but for robust interpretations it is suggested to use these in combination with sequential changes in morphological and micromorphological features.

Pedogenesis and/or pedoplasmation differ on basalts as parent material and pyroclastic deposits as parent material. Researchers have demonstrated that soils formed on pyroclastic material have distinct micromorphological characteristics, which distinguish them from soils derived from other parent materials (Stoops et al., 2010, 2018; Stoops and Schaefer, 2018; Sedov et al., 2010 and references therein). Based on compilation of different studies, Stoops et al. (2010) showed that pedogenesis has different steps/stages for loose sediments/deposits and for coherent rocks. While the transformation of loose deposits (pyroclastic deposits in the present study) to soil is largely a matter of pedoturbation, the transformation of coherent rocks (basalt in the present study) to soil involves two subsequent steps. In the latter case, first step results in formation of saprolite through weathering of rock and the second step involves pedoplasmation of saprolite resulting in formation of soil. However, the nature of saprolite depends on the type of bedrock and saprolites are shallow to non-existent on quartz-free calcareous, basaltic and mafic lithologies (Zauyah et al., 2010; Stoops et al., 2010 and references therein). Nonetheless, pedoplasmation is expressed by disappearance of the original rock fabric, development of microstructure and porosity, and development of other changes in micromorphological features (e.g. b-fabrics) on a given parent material (Stoops et al., 2010). Further, sequential development of micromorphological features occurs with advancement in pedogenesis under a given set of climatic conditions and environmental set-up (Stoops et al., 2010). This becomes more important in soils formed on pyroclastic deposits. Tephra in particular differs from several other parent materials not only in mineralogical composition, but also by their layering due to periodic changes in pyroclast deposition (Stoops et al., 2010).

Identified coarse material in the palaeosol profile clearly suggest formation of soil on pyroclastic material. The coarse fraction consists of pyroclastic material predominantly comprising scoria/sideromelane, and basaltic glass/glass shards along-with tachylite and some plagioclase laths. Also, extremely weathered/altered grains and fresh grains co-exist in a single horizon (in Bwb1, Bwb2, Bwb3). This is a common feature in volcanic ash soils (Stoops et al., 2010, 2018). Pedogenesis, in particular bioturbation continues along-with addition of fine pyroclastic material. Certainly, the rate of pedogenesis depends on the rate of pyroclast sedimentation. However, degree of abundance of a particular coarse material, its size range and percentage in altered to fresh coarse material varies from top to bottom in the profile. In general, there is increased component of very fine sand-size and fresh coarse material, for example from Bwb3 to topmost Bwb1. In particular, there is increase in abundance of glass shards, plagioclase laths and scoria grains in the top part of profile. The bottom-most horizon Bwb3) of profile shows lower proportion of coarse material and it largely consists of completely altered scoria with some moderately altered scoria, besides other completely altered coarse material and groundmass. However, there is absence of fresh plagioclase laths and glass shards. The geochemical weathering and pedogenic indices correlate well with the micromorphological observations. For example, this horizon shows highest CIW and clayeyness values in the bole bed profile. In general, coarse material decreases in size, from very coarse to fine sand size in the Bwb3 horizon to predominantly fine to very fine sand-size in the topmost Bwb1 horizon. This suggests that there is increase in addition of ash as pyroclastic material prior to occurrence of another phase of basalt lava flow.

Besides type of coarse material, various other distinct pedofeatures have been identified in the studied bole bed showing development of mature palaeosol on pyroclastic deposits, i.e. tephra. Mature soil formation indicates a significant duration of quiescence in flood basalt lava outpouring before emplacement of next lava flow. Based on the degree and nature of development of soil features in the buried palaeosol profile, the relative duration of quiescence and prevailing conditions can be explored. Development of pedogenic microstructure and voids form the first and the most important diagnostic pedoplasmation feature. The identified palaeosol profile shows development of granular microstructure throughout the profile, though blocky microstructure with weakly separated intrapedal granular microstructure predominates in the lower part of profile (the Bwb3 horizon). Pedogenesis on pyroclastic deposits during initial stage results in the formation of coarse monic basic microstructure, which progressively evolves to chito-enaulic followed by granular microstructure (Stoops et al., 2010). Thus, the identified volcanic palaeosol represents an advanced stage of pedogenesis based on identified microstructure.

Development of b-fabrics and its change during pedogenesis is another pedoplasmation feature (Stoops et al., 2010). The identified palaeosol shows predominantly undifferentiated b-fabric but at places speckled and weakly developed striated b-fabrics are present. The undifferentiated b-fabric is due to predominance of amorphous and cryptocrystalline colloidal components in soils formed on volcanic ash parent material (Kawai, 1969; Pain, 1971; Stoops et al., 2010). Sedov et al. (2010) documented that in volcanic ash soils where allophane is gradually replaced by crystalline clays, the micromass commonly shows an undifferentiated b-fabric, even when halloysite is abundant, but stipple-speckled b-fabrics have been described from soils containing kaolinite or illite. Spinola et al. (2017) interpreted that short periods of wet-dry cycles cause weakly developed granostriated and stipple-speckled b-fabrics in such bole bed palaeosols. Pedofeatures identified in the buried palaeosol profile indicate formation under warm, wet and well-drained conditions. And the dry cycles, if any occurred, were of limited duration maintaining sufficient soil moisture and were restricted in the topmost horizons. This is because there is absence of carbonate pedofeatures as well as any other specific pedofeatures indicative of significant wet-dry cycles characteristic of seasonal and/or arid climate. Also, absence of any significant redoximorphic pedofeatures in the palaeosol profile refute the presence of short- and/or long-term waterlogged conditions. The well-drained, oxidizing and acidic environment is further supported from the gleization, Ti/Al and U/Th values (Section 3.2). The warm wet climate and well-drained (i.e. oxygenated) conditions favoured diverse bioturbation and is evidenced based on presence of abundant faunal pedofeatures in the buried palaeosol profile. Though other sedimentary environments e.g. lacustrine can also undergo bioturbation, but in the present case bioturbation is pedoturbation based on association of other pedofeatures and absence of traces of primary sedimentary features/structures.

The topmost (15–25 cm) part of P2 layer, immediately below the basalt (B2) show heating effects of the overlying lava flow. In this case, effects of diagenetic processes due to circulation of hydrothermal fluids after burial of palaeosol surface by lava deposition are important to find out. It has been observed that the pedoplasmation features (e.g., faunal pedofeatures and granular microstructure) as identified through micromorphology have not undergone any significant changes except the filling of voids with glass. On contrary, there is significant variation in major basic cations in the topmost part of bole bed profile (Section 3.2. Thus, the lava flow resulted in geochemical rejuvenation by adding basic cations.

Characteristic microstructure, abundant and variety of voids alongwith faunal features including excrements are present in all the horizons of bole bed palaeosol profile. This indicates significant bioturbation of parent material by soil fauna. Spheroidal peds, in particular dominance of granular microstructure has been found in the studied palaeosol profile. Stoops et al. (2010, 2018) detailed how biological activity is mainly responsible for development of granular microstructure and more specifically the long-term termite activity. Further, oxic horizon, formed in particular on volcanic deposits, typically show a well-developed granular microstructure and formation of these aggregates could have been greatly aided by fungal activities (Stoops et al., 2010, 2018; Marcelino et al., 2010). However, some researchers have also postulated various other origins for the granular aggregates (Muller, 1983; Bitom and Volkoff, 1991; Eswaran and Daud, 1980; Stoops et al., 2010 and references therein). For example, physical origin involving mechanical fracturing due to alternating wetting and drying phases has been documented. Likewise, physico-chemical changes under extreme leaching conditions, wherein secondary role by soil mesofauna has been proposed by other researchers for the formation of granular aggregates (Stoops et al., 2010; Marcelino et al., 2010 and references therein). The most commonly reported and accepted origin for granular aggregates is the extensive biological activity. It is noteworthy that biological activities may be most common factors in the formation of granular peds/microstructure but the degree of development and its stability are related both to the climatic conditions and parent material composition (Marcelino et al., 2010). For example, several researchers have demonstrated that development and stability of granular microstructure is favoured under climates resulting in ustic soil moisture regimes and on parent material or soil having high gibbsite and iron-oxide contents. In the case of soils formed on volcanic materials (as parent material), the age of the soil also plays an important factor in granular microstructure stability and it is better-developed in older volcanic soils than the younger ones. Likewise, Bravard and Righi (1990) showed how slope position in a toposequence controls stability of granular microstructure.

In the studied Cretaceous age, buried volcanic soils, the Bwb1 and the Bwb2 horizons show granular peds with almost similar size, shape and structure indicating biological origin and the role of soil organisms e.g., termites, ants and mites (Stoops et al., 2010, 2018). Also, such soil fauna has close association with the micro-organisms e.g., fungi and bacteria, and these organisms are predominantly responsible for decomposing dead leaves and other organic matter. Another line of evidence for biological origin is the absence of polyhedral shape granular peds, which are formed by cracking of soil material due to alternating wet and dry conditions (Cooper et al., 2005). Besides granular microstructure, different void types ranging from planar, channel, chamber and irregular vugh have been identified in the palaeosol profile indicating significant bioturbation. Above all, planar voids present in the Bwb2 and the Bwb3 horizons are largely unaccommodating and rough in nature, thereby suggesting role of soil fauna. Presence of abundant faunal excrements suggest high activity of mesofauna. Plant residues were not observed in any of the buried Bw horizons. One of the possible explanations for scarce preservation of plant residues is due to an overall stronger oxidizing environment under high temperature and acidic soil conditions, which is well corroborated by geochemical results. Besides, the oganic matter/plant decomposition occurred rapidly due extensive microbial and faunal activity as observed from a number of faunal pedofeatures including degraded plastered channels, chambers, and unaccommodating, rough planar voids as well as organo-mineral complexes of spheroidal peds. Though some coatings and hypocoatings of micromass material and alteration products have been observed, no illuvial laminated coatings were found in the bole bed palaeosol profile. To be specific, spheroidal peds are predominant and the faunal pedofeatures are most developed than all other pedofeatures.

5. Conclusions

i. Systematic, in-depth micromorphology demonstrate that the investigated buried bole bed profile were mature palaeosols formed on pyroclastic deposits.
ii. Significant biodiversity under ustic soil moisture regimes existed and resulted in the formation of ferralsols.
iii. A greater impact of andosolization on ferralsols is interpreted before onset of successive basalt lava flow.
iv. The combination of morphological, micromorphological and geochemical results indicate presence of oxidizing environment under high temperature and acidic soil conditions during pedogenesis.
v. Systematic bole bed micromorphology is pre-requisite for understanding of surficial conditions during quiescence in volcanism.

CRediT authorship contribution statement

Seema Singh: Writing – original draft, Visualization, Validation, Supervision, Project administration, Methodology, Investigation, Data curation, Conceptualization. **Ajay Kumar:** Visualization, Methodology, Formal analysis, Data curation. **Soumyajit Mukherjee:** Writing – review & editing, Investigation, Conceptualization. **Charu Sharma:** Methodology, Formal analysis, Data curation. **Anshul Dhiman:** Methodology, Formal analysis, Data curation.

Declaration of competing interest

The authors declare that they have no known competing financial interests or personal relationships that could have appeared to influence the work reported in this paper.

Acknowledgements

The authors SS, AK, CS and AD are thankful to the Chairperson, Department of Geology, Panjab University, Chandigarh (India) for providing necessary facilities whereas the author SM is thankful to the Head of the Department of Earth Sciences, Indian Institute of Technology Bombay (India) for necessary facilities. Special thanks are due to late Prof. Georges Stoops (Ghent University, Belgium) for his preliminary guidance in the profile thin-sections. We thank the Handling Editor/s and the reviewer(s) for critical comments and suggestions which greatly improved the quality of this article.

Appendix A. Supplementary data

Supplementary data to this article can be found online at https://doi.org/10.1016/j.catena.2025.108797.

References

Bandemer, S.L., Schaible, P.J., 1944. Determination of iron. A study of the o-phenanthroline method. Ind. Eng. Chem. Anal. Ed. 16, 317–319. https://doi.org/10.1021/i560129a013.

Barrón, V., Torrent, J., 2002a. Evidence for a simple pathway to maghemite in Earth and Mars soils. Geochim. Cosmochim. Acta 66, 2801–2806.

Barrón, V., Torrent, J., 2002b. Diffuse reflectance spectroscopy of iron oxides. Encyclopedia of surface and Colloid Science 1, 1438–1446pp.

Beane, J.E., Turner, C.A., Hooper, P.R., Subbarao, K.V., Walsh, J.M., 1986. Stratigraphy, composition and form of the Deccan basalts, western Ghats, India. Bull. Volcanol. 48, 61–83.

Birkeland, P.W., 1984. Soils and geomorphology. Oxford University Press.

Bitom, D., Volkoff, B., 1991. Mise en évidence de deux modes de microstructuration dans une couverture de sols ferralitiques rouges du Sud-Cameroun. Science Du Sol 29, 289–300.

Bondre, N., Hart, W., Sheth, H., 2006. Geology and geochemistry of the Sangamner mafic dike swarm, western Deccan volcanic province, India: implications for regional stratigraphy. J. Geol 114, 155–170.

Bravard, S. and Righi, D., 1990. Micromorphology of an oxisol-spodosol catena in Amazonia (Brazil). In Developments in soil science (Vol. 19, pp. 169-174). Elsevier.

Carver, R.E., 1971. Holocene and Late Pleistocene sediment sources, continental shelf off Brunswick, Georgia. J. Sedimentary Res. 41 (2), 517–525.

Condie, K.C., Dengate, J., Cullers, R.L., 1995. Behavior of rare earth elements in a paleoweathering profile on granodiorite in the Front Range, Colorado, USA. Geochim. Cosmochim. Acta 59, 279–294.

Cooper, M., Vidal-Torrado, P., Chaplot, V., 2005. Origin of microaggregates in soils with ferralic horizons. Sci. Agric. 62, 256–263.

Courtillot, V., Gaudemer, Y., 1996. Effects of mass extinctions on biodiversity. Nature 381 (6578), 146–148.

Craig, P., Chevrier, V., Sayyed, M.R.G., Islam, R., 2017. Spectral analysis of Deccan intrabasaltic bole beds: implications for the formation and alteration of phyllosilicates on Mars. Planet. Space Sci. 135, 55–63.

Dhiman, A., Singh, S., Mukherjee, S., 2024. Micromorphology of basalt alterite and its implications on the geological processes during quiescence period of the Deccan volcanism, Kharghar hill, Maharashtra, India. J. Indian Assoc. Sedimentol. 41 (II), 32–39. https://doi.org/10.51710/jias.v41iII.377.

Duraiswami, R.A., Das, S., Shaikh, T.N., 2012. Hydrogeological framework of Aquifers in the Deccan Traps, India: some insights. In: Pawar, N.J., Das, S., Duraiswami, R.A. (Eds.), Hydrogeology of Deccan Traps and Associated Formations in Penninsular India. Geol Soc India, Bangalore.

Eggins, S.M., 2007. Laser Ablation ICP-MS Analysis of geological materials prepared as lithium borate glasses. Geostand. Newslett.

Ernst, R.E., 2014. Large igneous provinces. Cambridge University Press.

Eswaran, H., Daud, N., 1980. A scanning electron microscopy evaluation of the fabric and mineralogy of some soils from Malaysia. Soil Sci. Soc. Am. J. 44, 855–861.

Federoff, N., Courty, M.-A., Guo, Z., 2010. Palaeosols and relict soils. In: Interpretation of Micromorphological Features of Soils and Regoliths (ed. G. Stoops, V. Mercelino and F. Mees), 623 – 662. Amsterdam: Elsevier.

Fedo, C.M., Wayne Nesbitt, H., Young, G.M., 1995. Unraveling the effects of potassium metasomatism in sedimentary rocks and paleosols, with implications for paleoweathering conditions and provenance. Geology 23 (10), 921–924.

Gavin, P., 2012. Stability of phyllosilicates on Mars. University of Arkansas.

Gavin, P., Chevrier, V., Sayyed, M.R.G. and Islam, R., 2010, March. Spectral analysis of Deccan paleosols, India: Analog for phyllosilicates on Mars. In 41st Annual Lunar and Planetary Science Conference (No. 1533, p. 1904).

Gérard, M., Caquineau, S., Pinheiro, J., Stoops, G., 2007. Weathering and allophane neoformation in soils on volcanic ash from the Azores. European Journal of Soil Science 58, 496–515.

Ghodke, S.S., 1979. Geology of the area around Panvel, Kolaba District, Maharashtra. Poona University, Pune. Ph. D. Thesis.

Ghosh, P., Sayeed, M.R.G., Islam, R., Hundekari, S.M., 2006. Inter-basaltic clay (bole bed) horizons from Deccan traps of India: Implications for palaeo-weathering and palaeo-climate during Deccan volcanism. Palaeogeogr. Palaeoclimatol. Palaeoecol. 242 (1–2), 90–109.

Greenberger, R.N., Mustard, J.F., Kumar, P.S., Dyar, M.D., Breves, E.A., Sklute, E.C., 2012. Low temperature aqueous alteration of basalt: Mineral assemblages of Deccan basalts and implications for Mars. J. Geophys. Res. Planets 117 (E11).

Haggerty, B.M., 1996. Episodes of flood-basalt volcanism defined by 40Ar/39Ar age distributions: correlation with mass extinctions. J. Undergraduate Res. 3, 155–164.

Harnois, L., 1988. The CIW index: a new chemical index of weathering. Sed. Geol. 55 (3), 319–322.

Jongerius, A. and Heintzberger, G., 1975. Methods in soil micromorphology: a technique for the preparation of large thin sections (No. 10). Stichting voor Bodemkartering Wageningen.

Kawai, K., 1969. Changes in cation exchange capacity of some Andosols with dithionite-citrate treatment. Soil Sci. Plant Nutr. 15 (3), 97–103.

Kletetschka, G., Wasilewski, P.J., Taylor, P.T., 2000. Mineralogy of the sources for magnetic anomalies on Mars. Meteorit. Planet. Sci. 35 (5), 895–899.

Li, Y.H., 2000. A compendium of geochemistry. Princeton university press, princeton, New Jersey.

Mahoney, J.J., 1988. Deccan Traps. In: Macdougall, J.D. (Ed.), Continental Flood Basalts. Kluwer Acd. Pub, Holland, pp. 151–194pp.

Marcelino, V., Stoops, G., Schaefer, C.E.G.R., 2010. Oxic and related materials. In: Stoops, G., Marcelino, V., Mees, F. (Eds.), Interpretation of Micromorphological Features of Soils and Regoliths. Elsevier, Amsterdam, pp. 305–327.

Maynard, J.B., 1992. Chemistry of modern soils as a guide to interpreting Precambrian paleosols. J. Geol. 100 (3), 279–289.

McLean, D.M., 1985. Deccan Traps mantle degassing in the terminal Cretaceous marine extinctions. Cretac. Res. 6 (3), 235–259.

Miedema, R., Pape, T., Van der Waal, G.J., 1974. A method to impregnate wet soil samples, producing high-quality thin sections. Neth. J. Agr. Sci. 22, 37–39.

Misra, A.A., Bhattacharya, G., Mukherjee, S., Bose, N., 2014. Near N–S paleo-extension in the western Deccan region, India: Does it link strike-slip tectonics with India–Seychelles rifting? Int J Earth Sci (geol Rundsch) 103, 1645–1680.

Mukherjee, S., Misra, A.A., Calvès, G. and Nemčok, M., 2017. Tectonics of the Deccan large igneous province: An introduction. In: Mukherjee, S., Misra, A.A., Calvès, G. and Nemčok, M., (Eds) Geological Society, London, Special Publications, 445(1), pp.1-9.

Muller, J.P., 1983. Micro-organization of loose ferralitic materials in the Cameroons. In Bullock, P. & Murphy, C.P. (eds.), Soil Micromorphology. Volume 2. Soil Genesis. AB Academic Publishers, Berkhamsted, UK, pp. 655–666.

Munsell, 2000. Munsell Soil Colour Charts. Gretag Macberth, New York.

Olsen, P.E., 1999. Giant lava flows, mass extinctions, and mantle plumes. Science 284 (5414), 604–605.

Pain, L.F., 1971. Micromorphology of soils developed from volcanic ash and river alluvium in the Kohada Valley, Northern District, Papua. J. Soil Sci. 22, 275–280.

Prasad, R.V., Singh, N.D., Singh, S.K., Jain, V., 2025. Factors controlling basalt weathering in the Deccan traps: A small catchment perspective. Catena 249, 108566.

Rampino, M.R., Stothers, R.B., 1988. Flood basalt volcanism during the past 250 million years. Science 241 (4866), 663–668.

Retallack, G.J., Reinhardt, J., Sigleo, W.R., 1988. Field recognition of paleosols. Geol. Soc. Am. Spec. Pap. 216, 1–20.

Ruxton, B.P., 1968. Measures of the degree of chemical weathering of rocks. J. Geol. 76 (5), 518–527.

Rye, R., Holland, H.D., 2000. Geology and geochemistry of paleosols developed on the Hekpoort basalt, Pretoria Group. South Africa. American Journal of Science 300 (2), 85–141.

Sayyed, M.R.G., Hundekari, S.M., 2006. Preliminary comparison of ancient bole beds and modern soils developed upon the Deccan volcanic basalts around Pune (India): Potential for palaeoenvironmental reconstruction. Quat. Int. 156, 189–199.

Sayyed, M.R.G., 2014. Flood basalt hosted palaeosols: Potential palaeoclimatic indicators of global climate change. Geosci. Front. 5 (6), 791–799.

Sedov, S., Stoops, G., Shoba, S., 2010. Regoliths and Soils onVolcanic Ash. In: Stoops, G., Marcelino, V., Mees, F. (Eds.), Interpretation of micromorphological features of soils and regoliths. Elsevier, pp. 275–296pp.

Self, S., Thordarson, T., Keszthelyi, L., 1997. Emplacement of continental flood basalt lava flows. Geophysical Monograph-American Geophysical Union 100, 381–410.

Shapiro, Leonard, 1975. Rapid analysis of silicate, carbonate, and phosphate rocks revised edition: U.S. Geological Survey Bulletin 1401, pp. 76.

Sheldon, N.D., Tabor, N.J., 2009. Quantitative paleoenvironmental and paleoclimatic reconstruction using paleosols. Earth Sci. Rev. 95 (1–2), 1–52.

Sheldon, N.D., 2003. Pedogenesis and geochemical alteration of the Picture Gorge subgroup, Columbia River basalt. Oregon. Geological Society of America Bulletin 115 (11), 1377–1387.

Shrivastava, J.P., Ahmad, M., Srivastava, S., 2012. Microstructures and compositional variation in the intravolcanic bole clays from the eastern Deccan volcanic province: Palaeoenvironmental implications and duration of volcanism. J. Geol. Soc. India 80 (2), 177–188.

Singh, S., Parkash, B., Awasthi, A.K., 2015. Tectono-geomorphic and environmental set-up deduced during deposition of Mio-Pleistocene sediments in NW Himalaya, India. Catena 126, 173–188.

Singh, P., Banerjee, S., Pande, K., Bhattacharya, S., Sarkar, S., Le Perra, E., 2022. Authigenic Green Mica in Interflow Horizons within Late Cretaceous Deccan Volcanic Province, India and Its Genetic Implications. Minerals 12 (2), 198. https://doi.org/10.3390/min12020198.

Singh, S., Ghosh, P., Khanna, Y., 2017. Need for re-apprehension of basin tectono-depositional set-up during initial stage of Himalayan orogeny from pedogenic evidences. Catena 156, 102–112.

Singh, P., Le Pera, E., Bhattacharya, S., Pande, K., Banerjee, S., 2021. Mineralogical and textural characteristics of red boles of western Deccan volcanic province, India: Genetic and paleoenvironmental implications. A Multi-Proxy Approach, Mesozoic Stratigraphy of India, pp. 697–722.
Soil Survey Staff, 1992. Key to Soil Taxonomy: Soil Management. Support Services Monograph No. 19. Pocahontas Press, Blacksburg, pp. 541.
Spinola, D.N., de Castro Portes, R., Schaefer, C.E.G.R., Solleiro-Rebolledo, E., Pi-Puig, T., Kühn, P., 2017. Eocene paleosols on King George Island, Maritime Antarctica: macromorphology, micromorphology and mineralogy. Catena 152, 69–81.
Srivastava, P., Sangode, S.J., Torrent, J., 2015. Mineral magnetic and diffuse reflectance spectroscopy characteristics of the Deccan volcanic bole beds: Implications to genesis and transformations of iron oxides. Geoderma 239, 317–330.
Srivastava, P., Sangode, S.J., Meshram, D.C., Gudadhe, S.S., Nagaraju, E., Kumar, A., Venkateshwarlu, M., 2012. Paleoweathering and depositional conditions in the inter-flow sediment units (bole beds) of Deccan Volcanic Province, India: a mineral magnetic approach. Geoderma 177, 90–109.
Srivastava, P., Siddaiah, N.S., Sangode, S.J., Meshram, D.C., 2018. Mineralogy and geochemistry of various colored boles from the Deccan volcanic province: implications for paleoweathering and paleoenvironmental conditions. Catena 167, 44–59.
Sriwastava, P., Singh, V.V., Mathew, G., Kogure, T., Myneni, S., 2023. Origin of clays in the interbasaltic red boles of Deccan Volcanics: Pedogenesis versus palagonitization. Appl. Clay Sci. 246, 107183.
Stoops, G., 2003. Guidelines for the Analysis and Description of Soil and Regolith Thin Sections. SSSA, Madison., p. 184
Stoops, G., 2021. Guidelines for the Analysis and Description of Soil and Regolith Thin Sections. ACSESS, 2nd Edition.
Stoops, G., Marcelino, V., Mees, F., 2018. Interpretation of micromorphological features of soils and regoliths. Elsevier, p. 982pp.
Stoops, G., Schaefer, C.E., 2018. Pedoplasmation: formation of soil material. In Interpretation of micromorphological features of soils and regoliths. Elsevier, pp. 59–71.
Stoops, G., Marcelino, V., Mees, F., 2010. Micromorphological features and their relation to processes and classification: general guidelines and keys. In Interpretation of micromorphological features of soils and regoliths. Elsevier, pp. 15–35.
Wänke, H., Brückner, J., Dreibus, G., Rieder, R., Ryabchikov, I., 2001. Chemical composition of rocks and soils at the Pathfinder site. In Chronology and Evolution of Mars: Proceedings of an ISSI Workshop, 10–14,, April 2000. Bern, Switzerland. Springer, Netherlands, pp. 317–330.
White, R.V., Saunders, A.D., 2005. Volcanism, impact and mass extinctions: incredible or credible coincidences? Lithos 79 (3–4), 299–316.
Widdowson M, Walsh J N, and Subbarao K V 1997 The geochemistry of Indian bole horizons: Palaeoenvironmental implications of Deccan intravolcanic palaeosurfaces; In: Palaeosurfaces: Recognition, reconstruction and palaeoenvironmental interpretation (ed.) Widdowson M, Geol. Soc. Spec. Publ. **120** 269–281.
Wignall, P.B., 2001. Large igneous provinces and mass extinctions. Earth Sci. Rev. 53 (1–2), 1–33.
Wilkins A, Subbarao K B, Ingram G, and Walsh J N 1994 Weathering regimes within the Deccan Basalts; In: Volcanism (ed.) Subbarao K, Wiley Eastern Ltd., pp. 217–231.
Zauyah, S., Schaefer, C.E., Simas, F.N., 2010. Saprolites. In Interpretation of micromorphological features of soils and regoliths. Elsevier, pp. 49–68.